



ELSEVIER

Contents lists available at ScienceDirect

## Sensors and Actuators B: Chemical

journal homepage: [www.elsevier.com/locate/snb](http://www.elsevier.com/locate/snb)

## Lossy mode resonance sensors based on nanocoated multimode-coreless-multimode fibre

Adrian Vicente<sup>a</sup>, Desiree Santano<sup>a</sup>, Pablo Zubiate<sup>a</sup>, Aitor Urrutia<sup>a,b</sup>, Ignacio Del Villar<sup>a,b,\*</sup>, Carlos Ruiz Zamarreño<sup>a,b</sup><sup>a</sup> Electrical, Electronic and Communications Engineering Department, Public University of Navarra, 31006, Pamplona, Spain<sup>b</sup> Institute of Smart Cities (ISC), Public University of Navarra, 31006, Pamplona, Spain

## ARTICLE INFO

## Keywords:

Optical fibre sensor  
Resonance  
Thin-film  
Refractometer  
Biosensor

## ABSTRACT

In this work it is proved the ability to obtain lossy mode resonances (LMRs) in the transmission spectrum with multimode-coreless-multimode fibre optic structure coated with tin oxide on the coreless segment. The devices were characterized as a function of the surrounding medium refractive index and sensitivities of 7346.93 nm/RIU and 708.57 nm/RIU were attained for the first and the second LMR respectively. As an application proof of this technology, one of the devices was biofunctionalized and used for detecting goat anti-mouse IgG in concentrations ranging from 1 to 40 mg/L, with a limit of detection of 0.6 mg/L. This proves the ability of this simple structure to be used for biological, chemical or environmental applications.

## 1. Introduction

The combination of optical fibre and nanomaterials provides a good platform for the development of sensors that can be applied in a wide range of domains, such as industry, medicine, biology or chemistry [1]. All these applications are possible thanks to the fine properties of optical fibre: immunity against electromagnetic interferences, small size, reduced cost and capability of remote sensing and wavelength multiplexing.

The utilization of nanostructures permits to obtain high sensitivity values in what can be called a lab-on-fibre [2], which has been exploited by many authors in literature using many different optical fibre configurations, such as fibre Bragg gratings (FBGs) [3,4], long-period gratings (LPGs) [5,6] and interferometers [7,8]. Among them, interferometers, due to their simplicity of fabrication, have been used for the development of a wide range of sensing applications providing high-resolution measurements due to their capability of developing prominent attenuation/transmission bands [8]. Different kinds of interferometric structures can be distinguished, such as Fabry-Perot interferometer (FPI), Mach-Zehnder interferometers (MZIs), Michelson interferometers, Sagnac interferometers and very simple interferometric structures like single mode-coreless-single mode fibre (typically called SMS because sometimes the coreless segment is called multimode segment) and multimode-coreless-multimode fibre (MCM) [9]. In the latter structures, the coreless segment permits the evanescent field of

modes to interact with the outer medium. As a result, the transmission and attenuation bands experience a wavelength shift as a function of the surrounding medium refractive index (SMRI) or the thin-film thickness [7].

In comparison with the SMS structure, the MCM structure couples more light from the coreless segment to the multimode fibre because the diameter of a multimode fibre is wider than that of a single-mode fibre. In particular, ref. [10] explores the influence of the multimode segment for generating attenuation/transmission bands. In addition, the presence of a thin-film on a coreless fibre has been used for generating lossy mode resonances (LMRs), a phenomenon that is characteristic of metallic oxide nanocoated optical fibre sensors [11–17].

Another important factor in the performance of LMR based optical fibre sensors is the thin-film refractive index material, which determines the sensitivity of the device [13]. In this regard, the highest sensitivity has been attained with tin oxide [18]. Consequently, this material will be used for the analysis developed in this work.

In this paper, two applications will be developed to assess the performance of thin-film coated MCM based LMR sensors: a refractometer and a biosensor. The first and the second LMR will be analyzed both in the visible and near infrared regions for the refractometric application, whereas the binding affinity between mouse IgG and goat anti-mouse IgG will be tested with the biosensor.

\* Corresponding author at: Electrical, Electronic and Communications Engineering Department, Public University of Navarra, 31006, Pamplona, Spain.

E-mail address: [ignacio.delvillar@unavarra.es](mailto:ignacio.delvillar@unavarra.es) (I. Del Villar).<https://doi.org/10.1016/j.snb.2019.126955>

Received 17 April 2019; Received in revised form 2 August 2019; Accepted 6 August 2019

0925-4005/© 2019 Elsevier B.V. All rights reserved.

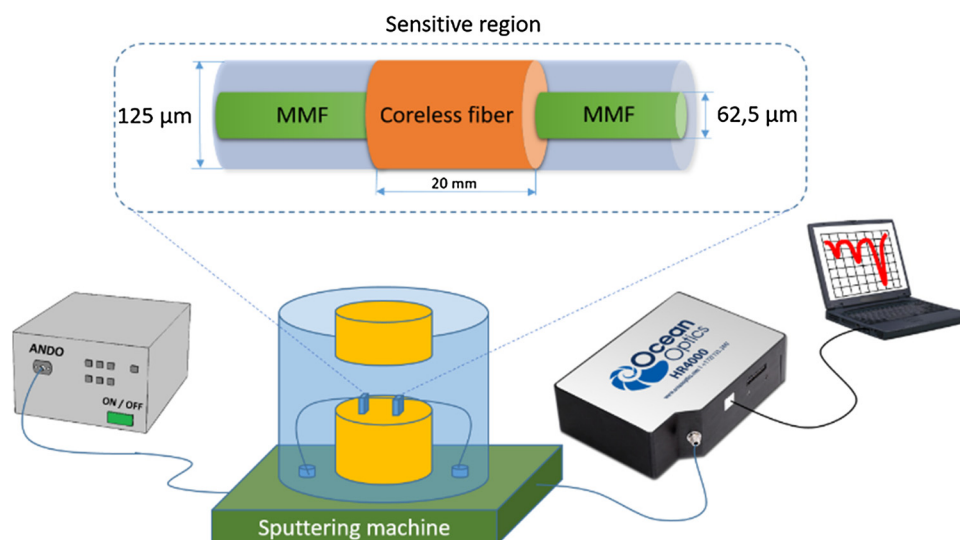


Fig. 1. MCM structure and sputtering deposition setup.

## 2. Method and materials

The MCM structure, described in Fig. 1, consists of two standard multimode optical fibre pigtailed (Phoenix photonics MMF, core diameter 62.5  $\mu\text{m}$ , cladding diameter 125  $\mu\text{m}$ , connectors FC/PC) fused at both sides of a coreless optical fibre segment of diameter 125  $\mu\text{m}$  and length 20 mm from POFC Inc. (Taiwan).

The coreless section of the MCM structure (i.e. the sensitive region) was coated with a thin film of black tin oxide ( $\text{SnO}_{2-x}$ ) using a sputtering machine K675XD from Quorum Technologies, Ltd. (for the sake of simplicity instead black tin oxide we will use the term tin oxide henceforward). The parameters used in the experiment were  $8 \times 10^{-2}$  mbar argon partial pressure and 90 mA of current intensity.

The fabrication of the  $\text{SnO}_{2-x}$  thin film was monitored using the setup shown in Fig. 1, where a light source (Ando AQ-4303B) was connected to one end of the MCM optical fibre and the other end was connected to a spectrometer (Ocean Optics Inc, HR 4000CG) to monitor the output power from 400 to 1000 nm.

The refractometric response of the  $\text{SnO}_{2-x}$  coated MCM as a function of the surrounding medium refractive index (SMRI) was tested by immersing the device in different refractive index solutions with the light source and the spectrometer shown in Fig. 1. To this purpose, different glycerol/water solutions were used, which corresponded with refractive indices 1.33, 1.34, 1.36, 1.38, 1.40, 1.42 and 1.44, measured with a refractometer (Mettler Toledo Inc, Refracto 30GS) operating at 589.3 nm.

In addition, an immunosensor application was tested with the experimental setup depicted in Fig. 2, where the  $\text{SnO}_{2-x}$  coated MCM structure is introduced in a thermo-stabilized flow-cell, which guarantees a constant temperature of  $26^\circ\text{C} \pm 0.01^\circ\text{C}$  (see Fig. 2). The contact between the lower part of the flow-cell, which is made of stainless steel, and two Peltier cells, allowed the temperature stabilization by a closed-loop control driven by a temperature controller (739-TC-14-PR-59, Laird Technologies/ Thermal Solutions). A NTC thermistor insulated lead 10k 2.19% was inserted into the stainless-steel piece in the vicinity of the flow channel. The whole system was mounted on a cooler in order to facilitate the temperature control. The upper part of the flow cell was made of ULTEM, a biocompatible and transparent material, where the coated MCM structure was placed and glued with a UV-polymerizing optical adhesive (NOA68, Norland Products Inc.). The flow cell was 80 mm long, 15 mm wide and 10 mm high. The flow channel consisted of a 1 mm wide, 0.5 mm deep and 50 mm long rectangular section groove that was built on the ULTEM and stainless-steel pieces. The upper part had two aligned holes with the flow channel as

inlet an outlet port for the fluid, which was inserted by a pump (Minipuls 3 peristaltic pump). In addition, the flow cell was completely sealed by using a parafilm membrane sandwiched between the upper and lower pieces.

The materials used for the functionalization procedure, the deposition of the biolayer procedure and the detection process are: methacrylic acid/methacrylate copolymer (Eudragit L100) from Evonik Degussa GmbH (Düsseldorf, Germany), mouse IgG (Prod 31903), goat anti-mouse-IgG (Prod A28174), 1-Ethyl-3-(3-dimethylaminopropyl) carbodiimide hydrochloride (EDC, Prod 22980) and N-hydroxysuccinimide (NHS, Ref 24500) from Thermofisher, human serum (C Reactive Protein Free Serum) from HyTest Ltd. (Turku, Finland), Bovine Serum Albumin (BSA, A2153-10 G) from Sigma Aldrich and PB (Phosphatebuffer, pH 7.4)

Different solutions were prepared with the previously mentioned products for the fabrication and testing of the biosensor: an EDC/NHS solution (2 mM/5 mM, respectively), a solution of IgG (5.7 mg/mL) in PB (40 mM), BSA (1%) in PB (40 mM) and several solutions with increasing concentrations of IgG in 1:10 serum diluted in PB.

## 3. Results

### 3.1. Fabrication of $\text{SnO}_{2-x}$ thin film and resonance characterization

The study presented in this section pursues the study of the LMR induced by a metallic oxide fabricated onto the MCM structure. In contrast to other works where the MCM structure is used for interferometric purposes [19] we use a shorter segment of 20 mm, which avoids the presence of the interferometric band. Thus, the LMR is generated in the same way that occurs in cladding removed 200  $\mu\text{m}$  core fibers [13]. Oppositely, in a previous publication that deals with the MCM structure [19], no LMR was induced because focus was centered in the study of the interferometric band and the thin-film thickness used is too low to induce an LMR. Therefore, the study of the LMR evolution as a function of the thin-film thickness is very important to characterize the device.

In order to characterize the evolution of the optical spectrum as a function of the coating thickness, it was monitored for 4 min with the conditions explained in Section 2. In Fig. 3 it is possible to observe the bands corresponding to the first and second LMR. According to previous publications [11,13], the wavelength shift ratio is higher for the first LMR than for the second LMR. Consequently, the aim will be to stop the deposition when the first LMR is located in the wavelength range monitored by the spectrometer. To this purpose, a second deposition

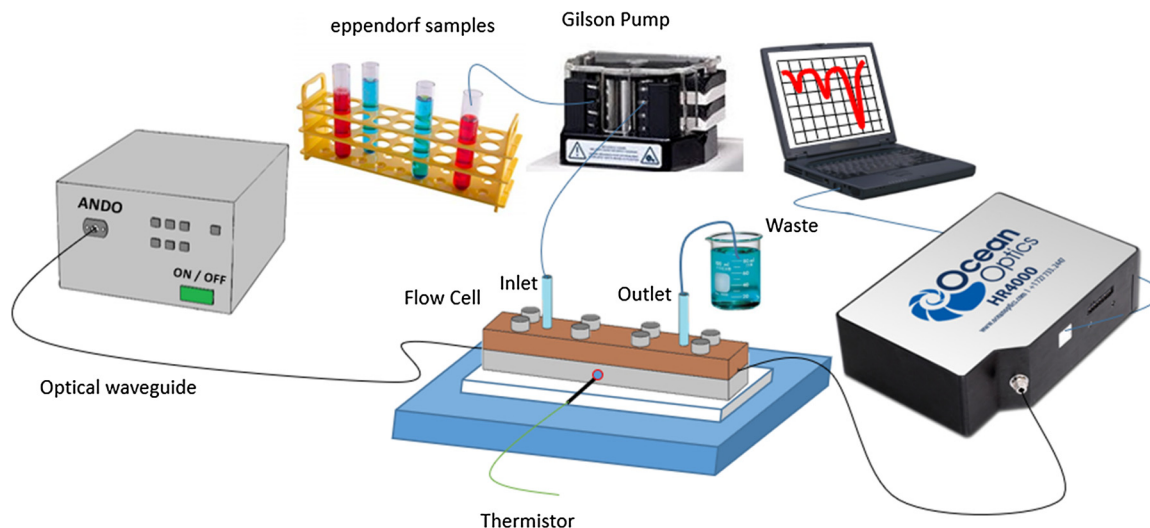


Fig. 2. Immunosensor setup.

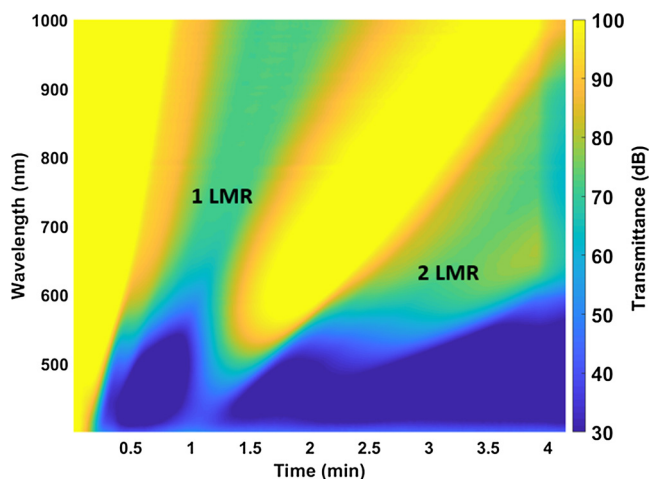


Fig. 3. Spectral response of the MCM device as a function of deposition time.

was performed on a new MCM structure stopping the fabrication process after 40 s, when the first LMR starts to be visualized in the optical spectrum working range.

The thickness of the nanocoatings deposited on both MCM structures was characterized with a field emission scanning electron microscope (model UltraPlus FESEM from Carl Zeiss Inc.) with an in-lens detector at 3 kV and an aperture diameter of 30  $\mu\text{m}$ . The results in Fig. 4a reveal that the nanocoating obtained after a 4 min deposition presented a thickness of 636 nm. Regarding the thinner nanocoating, obtained with a deposition of 40 s, its thickness was 82 nm (see Fig. 4b).

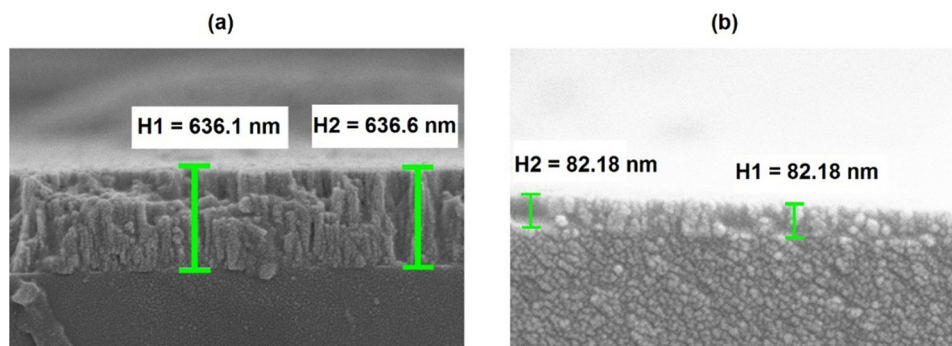


Fig. 4. Scanning electron microscope (SEM) images of a coreless section of the MCM device corresponding to deposition times: (a) 240 s and (b) 40 s.

### 3.2. Refractometer characterization

Prior to the refractometer characterization the obtained thin-films were measured using a UVISEL 2 (Horiba Inc.) ellipsometer, which revealed the refractive index model of the obtained films as it is shown in Fig. 5a. Here it is important to remark that the extinction coefficient ( $k$ ) is close to but not zero at long wavelengths. The model of the ellipsometer was used to obtain theoretically [11] the resonance wavelength for different surrounding medium refractive index as it is represented in Fig. 5b.

The fabrication of the device requires a precise control of the thin film thickness in order to position the first LMR within the operating wavelength range of the spectrometer in the range of refractive indices where the device will be used, whereas the large resonance width prevents from additional calculations, such as the figure of merit in this case. Fig. 6 shows the optical spectrum corresponding with the 82 nm coated MCM structure as a function of the SMRI in the range from 1.33 to 1.38, which corroborates the theoretical simulation obtained in Fig. 5(b). The interest of this range is that it includes water and other physiological fluids. Another sensor is analysed in Fig. 6 for the same SMRI range but it operates at longer wavelengths. To this purpose, it was deposited for a longer time: 75 s.

The curves obtained in Figs. 6(b) and 7 (b) for both resonances exhibit a non-linear behavior with a sensitivity increase for higher SMRIs. In particular, the sensor with the first LMR located at shorter wavelengths shows an average sensitivity of 3305.76 nm/RIU showing a sensitivity of 4604 nm/RIU when we take into account only higher SMRIs. On the other hand, the sensor with the first LMR located at longer wavelengths presents an average sensitivity of 7346.93 nm/RIU

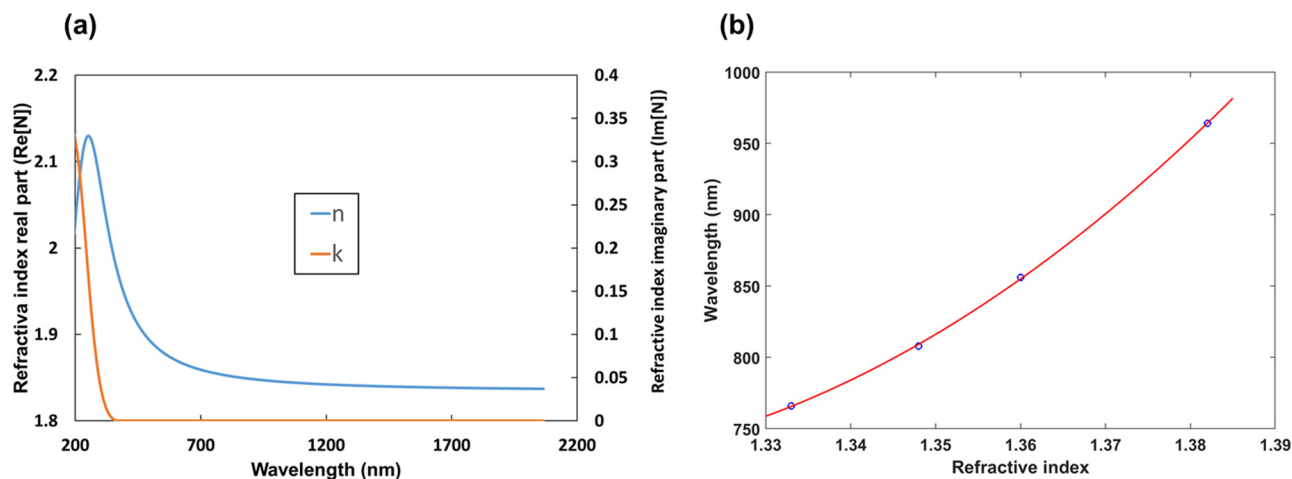


Fig. 5. (a) Refractive index real part and imaginary part of  $\text{SnO}_{2-x}$  thin-films obtained using UVISEL 2 ellipsometer. (b) Theoretical calculation of the resonance wavelengths of the MCM structure coated with a 82 nm thick  $\text{SnO}_{2-x}$  film and surrounded by different refractive indices.

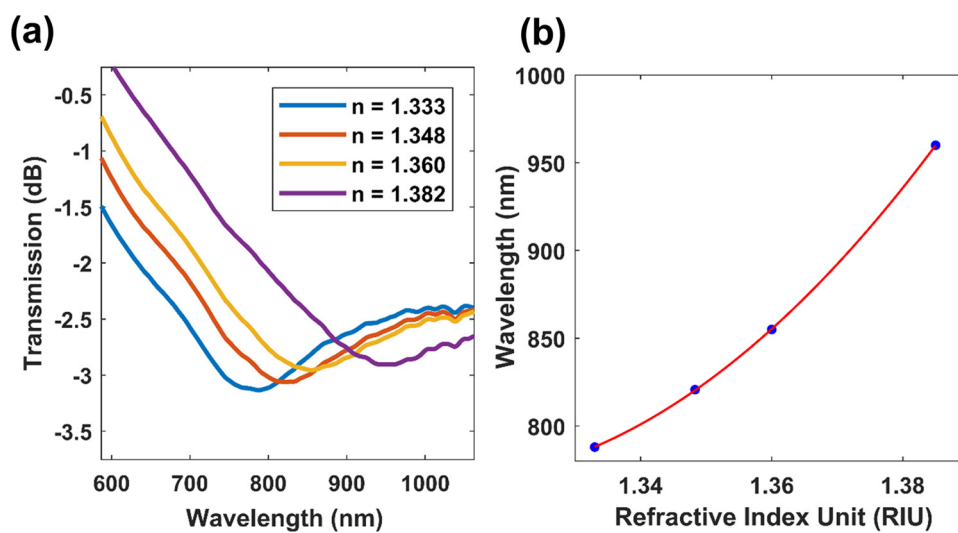


Fig. 6. MCM device deposited for 40 s (the first LMR is visible in a wavelength range from 400 to 1000 nm): (a) Transmission spectra for different SMRI values and (b) Resonance wavelength as a function of the SMRI.

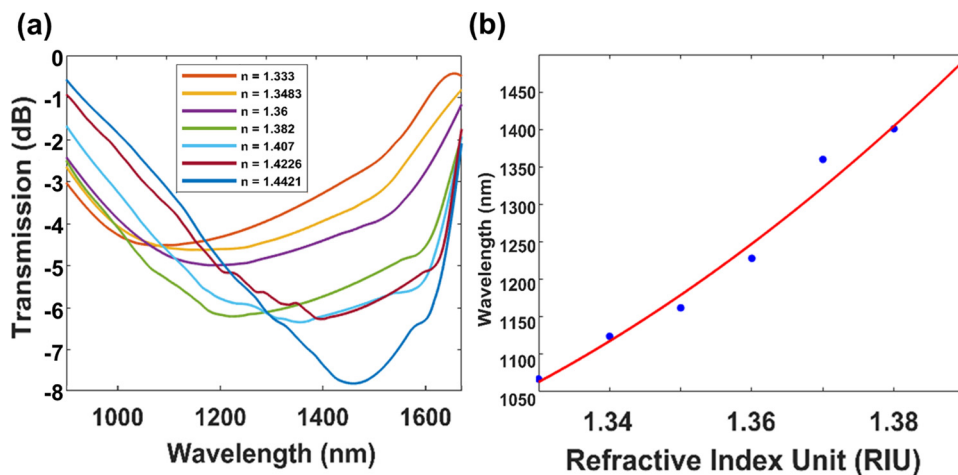


Fig. 7. MCM device deposited for 75 s (the first LMR is visible in a wavelength range from 1000 to 1700 nm): (a) Transmission spectra for different SMRI values and (b) Resonance wavelength as a function of the SMRI.

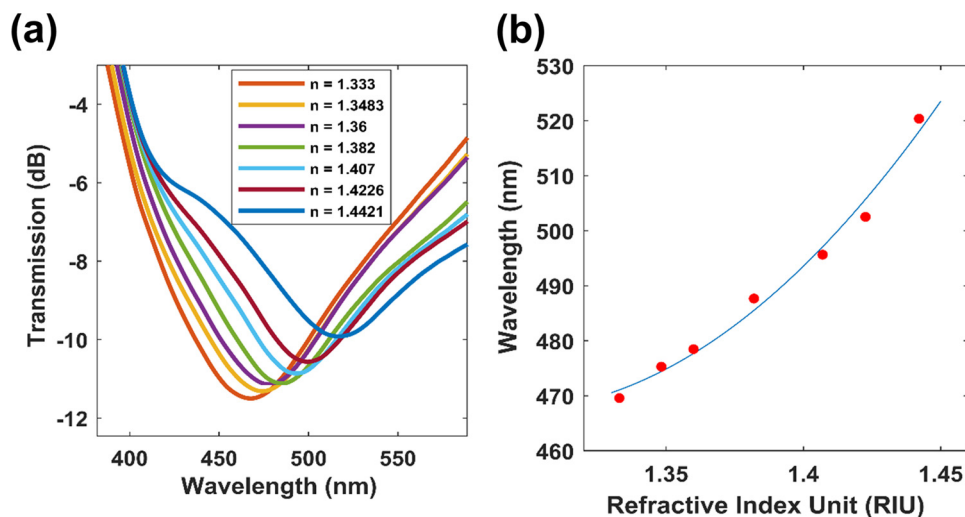


Fig. 8. MCM device deposited for 100 s (the second LMR is visible at a wavelength range from 400 to 1000 nm): (a) Transmission spectra for different SMRI values and (b) Resonance wavelength as a function of the SMRI.

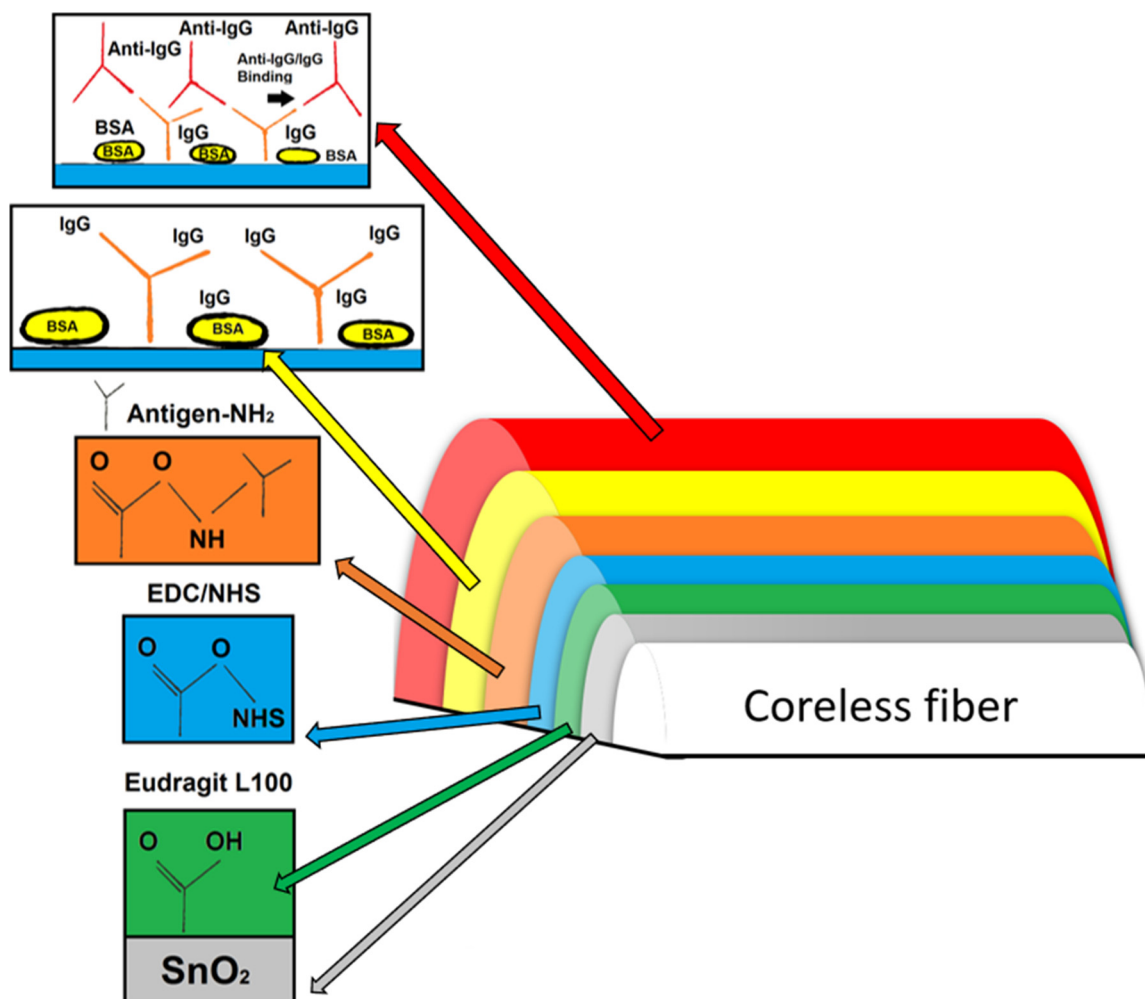


Fig. 9. Schematic representation of the biosensor structure after the functionalization procedure, the deposition of the biolayer procedure and the detection process.

showing a sensitivity of 9818.18 nm/RIU when we take into account only the highest SMRIs.

For the sake of comparison, a third device with deposition time 100 s was fabricated to analyse the second LMR in the short wavelength range as a function of refractive index (Fig. 8). The sensitivity,

according to design rules for LMR based sensors is lower than the first LMR [13], with an average sensitivity of 466.05 nm/RIU and a sensitivity of 708.57 nm/RIU when we take into account the highest SMRIs.

**Table 1**  
Flow rates and times used in the biosensor application.

Sample	Flow rate ( $\mu\text{L}/\text{min}$ )	Time (min)
EDC/NHS	25	30
IgG	6	60
PB (washing step)	70	15
BSA	25	15
PB	170	15
Serum	4.25	15
Serum + Anti-IgG	4.25	15

### 3.3. Biosensor application

A biosensor was developed as an example of the applicability of the previous device. Here, the first LMR was monitored in order to obtain higher sensitivity than that obtained with the second LMR, as it was mentioned in the previous section. To this purpose, a new MCM structure was deposited with  $\text{SnO}_{2-x}$  with a deposition time that permitted to locate the first LMR in the short wavelength range, where optical equipment is less expensive. Then, the sensitive region of the sensor was immersed in 2 mM (0.04% w/v) Eudragit® L100 in ethanol for 1 min and subsequently dried in air for about 15 min until the solvent had been completely evaporated. This monolayer provided carboxylic functional groups ( $-\text{COOH}$ ) to the surface, useful for IgGs immobilization. The central wavelength of the LMR in air was 520 nm and it was shifted to longer wavelengths after the deposition of Eudragit and a further immersion of the sensor in liquid.

After the MCM functionalization using Eudragit®, the device was placed into the flow cell in order to fabricate the biolayer following the next steps: 1) activation of  $-\text{COOH}$  groups by means of EDC/NHS solution; 2) The immobilization of IgG on the MCM surface by pumping a solution of IgG in PB; and 3) a surface passivation with BSA in PB.

Once the biolayer was obtained, several solutions with increasing concentrations of IgG in serum diluted in PB were pumped into the flow cell. A washing stage of the flow cell using PB between each new IgG concentration (IgG from 1 mg/L to 40 mg/L) was necessary to determine the resonance wavelength shift associated to a new anti IgG binding onto the bilayer. The schematic representation of the biosensor structure after the functionalization procedure, the deposition of the biolayer procedure and the detection process is shown in Fig. 9, whereas a list of the flow rates and times spent in each of the solutions passed through the flow-cell is given in Table 1.

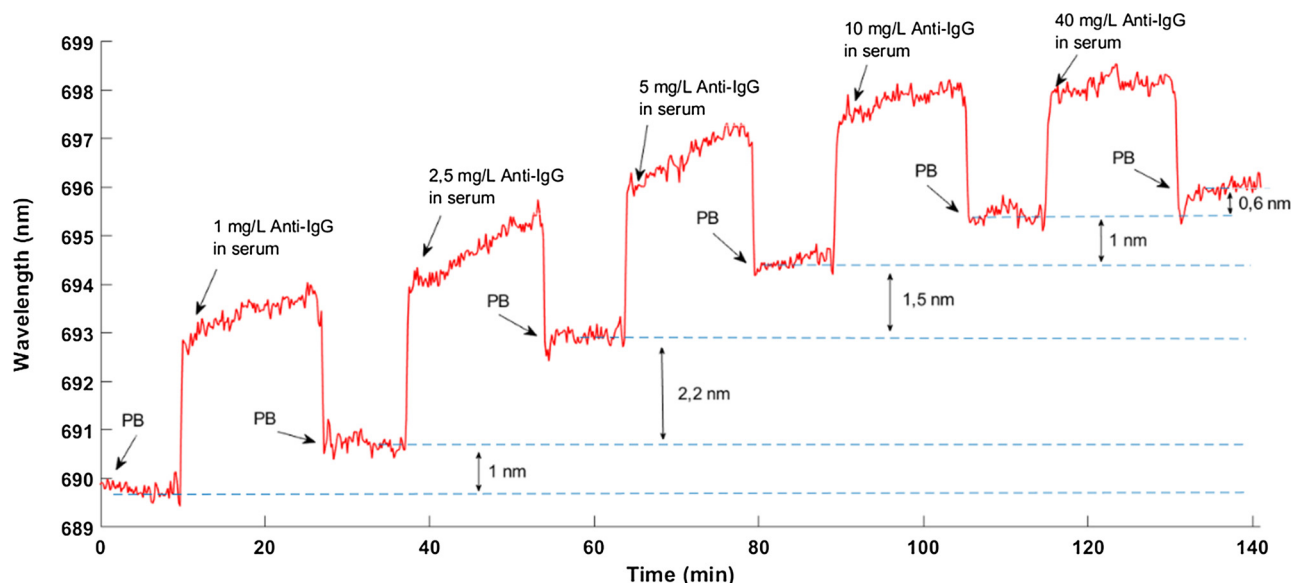


**Fig. 10.** Real time sensorgram with the evolution of the central wavelength of the first LMR.

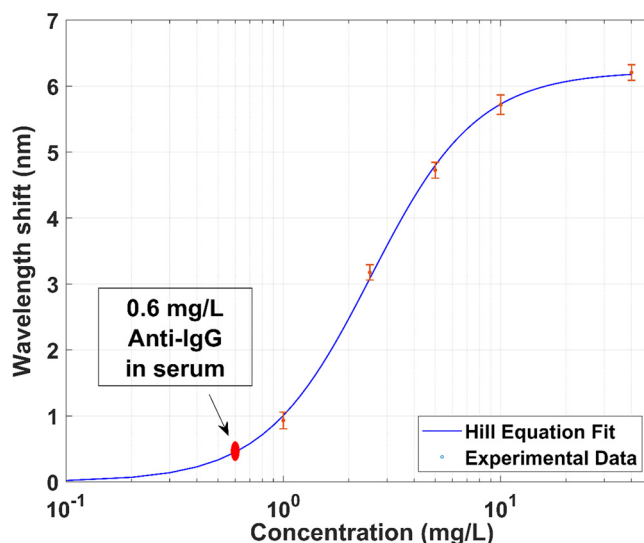


**Fig. 11.** Calibration curve of the biosensor.

A real time sensorgram with the evolution of the central wavelength of the first LMR is shown in Fig. 10, whereas the calibration curve with the wavelength shift of the LMR central wavelength in each concentration of anti-IgG is shown in Fig. 11 in a logarithmic scale. A Hill equation sigmoidal curve (blue curve) has been fitted with a correlation ( $R^2$ ) coefficient of 0.9997. According to this, a maximum standard deviation of 0.1475 is represented with red error bars and the limit of detection (LOD) achieved was 0.6 mg/L. The LOD can be obtained from the calibration curve through the inverse of the fitting Hill function evaluated in a well-defined point [20]. Since the LOD is related to both the sensitivity and the resonance width, i.e. the figure of merit [13,21,22], the value obtained is not very good compared to other works in literature that obtain femtomolar level detection [23]. However, the simplicity of the presented device compared to D-shaped fiber or other fiber optic setups could be a major advantage in some bio-sensing applications, though obviously the LOD is much higher due to the broad resonance.

#### 4. Conclusions

Tin oxide (SnO<sub>2-x</sub>), a metallic oxide with high refractive index, was deposited on multimode-coreless-multimode (MCM) structures to excite lossy mode resonances (LMRs). MCM structures with different coating thickness were fabricated, which allowed to obtain the first LMR and second LMR at wavelengths ranging from 400 to 1700 nm. The results obtained shown a sensitivity of 3305.76 nm/RIU for the first LMR between 400 and 1000 nm and a sensitivity of 7346.93 nm/RIU between 1000 and 1700 nm. On the other hand, by monitoring the second LMR it was observed a sensitivity reduction to 708.57 nm/RIU in the range 400–1000 nm.

In view of these results, and with the aim of monitoring the sensor at wavelength ranges where optical sources and detectors are less expensive, an application with the first LMR at short wavelengths was developed. To this purpose, the SnO<sub>2-x</sub> surface of one of the devices was biofunctionalized and fixed in a thermostabilized flow cell. Mouse IgGs were immobilized on the sensor surface and later it was possible to detect anti-mouse IgG in concentrations ranging from 1 to 40 mg/L with a LOD of 0.6mg/L. This proves that metallic oxide coated MCM structures can be used as an effective optical platform for biosensing, suitable for the development of portable, lightweight, high performance and cost-effective devices that can be used in many applications.

#### Acknowledgments

This work was supported in part by the Spanish Ministry of Education and Science FEDERTEC2016-78047, by the Government of Navarre through its projects with references: PC021-022 OPTISENS, BIOPTSENS AVANZA and 0011-1365-2017-000117 and by the Public University of Navarra PUN/UPNA26.

#### References

- [1] E. Udd, W.B. Spillman Jr., *Fiber Optic Sensors: an Introduction for Engineers and Scientists*, John Wiley & Sons, 2011.
- [2] P. Vaiano, B. Carotenuto, M. Pisco, A. Ricciardi, G. Quero, M. Consales, A. Crescitelli, E. Esposito, A. Cusano, Lab on fiber technology for biological sensing applications, *Laser Photon. Rev.* 10 (6) (2016) 922–961.
- [3] J. Albert, L.-Y. Shao, C. Caucheteur, Tilted fiber bragg grating sensors, *Laser Photon. Rev.* 7 (1) (2013) 83–108.
- [4] N. Kaplan, J. Jasenek, J. Červeňová, M. Ušáková, Magnetic optical fbg sensors using optical frequency domain reflectometry, *IEEE Trans. Magn.* 55 (1) (2019) 1–4.
- [5] F. Chiavaioli, P. Biswas, C. Trono, S. Jana, S. Bandyopadhyay, N. Basumallick, A. Giannetti, S. Tombelli, S. Bera, A. Mallick, et al., Sol-gel-based titania silica thin film overlay for long period fiber grating-based biosensors, *Anal. Chem.* 87 (24) (2015) 12024–12031.
- [6] L. Coelho, D. Viegas, J.L. Santos, J. De Almeida, Characterization of zinc oxide coated optical fiber long period gratings with improved refractive index sensing properties, *Sens. Actuators B Chem.* 223 (2016) 45–51.
- [7] Y. Cardona-Maya, Del Villar, A.B. Socorro, J.M. Corres, R. Mafias, J.F. Botero-Cadavid, Wavelength and phase detection based sms fiber sensors optimized with etching and nanodeposition, *J. Light. Technol.* 35 (17) (2017) 3743–3749.
- [8] X. Zhou, K. Chen, X. Mao, Q. Yu, et al., A reflective fiber-optic refractive index sensor based on multimode interference in a coreless silica fiber, *Opt. Commun.* 340 (2015) 50–55.
- [9] B.H. Lee, Y.H. Kim, K.S. Park, J.B. Eom, M.J. Kim, B.S. Rho, H.Y. Choi, Interferometric fiber optic sensors, *Sensors* 12 (3) (2012) 2467–2486.
- [10] Y. Jung, S. Kim, D. Lee, K. Oh, Compact three segmented multimode fibre modal interferometer for high sensitivity refractive-index measurement, *Meas. Sci. Technol.* 17 (5) (2006) 1129.
- [11] I. Del Villar, C.R. Zamarreño, M. Hernaez, F.J. Arregui, I.R. Matias, Lossy mode resonance generation with indium-tin-oxide-coated optical fibers for sensing applications, *J. Light. Technol.* 28 (1) (2010) 111–117.
- [12] S.P. Usha, S.K. Mishra, B.D. Gupta, Fiber optic hydrogen sulfide gas sensors utilizing ZnO thin film/ZnO nanoparticles: a comparison of surface plasmon resonance and lossy mode resonance, *Sens. Actuators B Chem.* 218 (2015) 196–214.
- [13] I. Del Villar, F.J. Arregui, C.R. Zamarreño, J.M. Corres, C. Barriain, J. Goicoechea, C. Elousa, M. Hernaez, P.J. Rivero, A.B. Socorro, et al., Optical sensors based on lossy-mode resonances, *Sens. Actuators B Chem.* 240 (2017) 174–185.
- [14] S.K. Mishra, S.P. Usha, B.D. Gupta, A lossy mode resonance-based fiber optic hydrogen gas sensor for room temperature using coatings of ITO thin film and nanoparticles, *Meas. Sci. Technol.* 27 (2016) 045103.
- [15] P. Zubiate, C.R. Zamarreño, I. Del Villar, I.R. Matias, F.J. Arregui, High sensitive refractometers based on lossy mode resonances (LMRs) supported by ITO coated D-shaped optical fibers, *Opt. Express* 23 (2015) 8045–8050.
- [16] M. Smietana, M. Sobaszek, B. Michalak, P. Niedzialkowski, W. Bialobrzaska, M. Koba, P. Sezemsky, V. Stranak, J. Karczewski, T. Ossowski, R. Bogdanowicz, Optical monitoring of electrochemical processes with ITO-based lossy-mode resonance optical fiber sensor applied as an electrode, *Journal of Lightwave Technology* 36 (4) (2016) 954–960.
- [17] D. Tiwari, K. Mullaney, S. Korposh, S.W. James, S.-W. Lee, R.P. Tatam, An ammonia sensor based on Lossy Mode Resonances on a tapered optical fibre coated with porphyrin-incorporated titanium dioxide, *Sens. Actuators B Chem.* 242 (2017) 645–652.
- [18] P. Sanchez, C.R. Zamarreño, M. Hernaez, I.R. Matias, F.J. Arregui, Optical fiber refractometers based on lossy mode resonances by means of SnO<sub>2-x</sub> sputtered coatings, *Sens. Actuators B Chem.* 202 (2014) 154–159.
- [19] N. San Fabián, A.B. Socorro-Leránz, I. Del Villar, S. Díaz, I.R. Matias, Multimode-Coreless-Multimode fiber-based sensors: theoretical and experimental study, *J. Lightwave Technol.* 37 (2019) 3844–3850.
- [20] F. Chiavaioli, C. Gouveia, P. Jorge, F. Baldini, Towards a uniform metrological assessment of gratingbased optical fiber sensors: from refractometers to biosensors, *Biosensors* 7 (2) (2017) 23.
- [21] C. Caucheteur, T. Guo, J. Albert, Review of plasmonic fiber optic biochemical sensors: improving the limit of detection, *Anal. Bioanal. Chem.* 407 (2015) 3883–3897.
- [22] A.B. Socorro-Leránz, D. Santano, I. Del Villar, I.R. Matias, Trends in the design of wavelength-based optical fibre biosensors, *Biosens. Bioelectron.* X 2008–2018 (2019) in press.
- [23] F. Chiavaioli, P. Zubiate, I. Del Villar, C.R. Zamarreño, A. Giannetti, S. Tombelli, C. Trono, F.J. Arregui, I.R. Matias, F. Baldini, Femtomolar detection by nanocoated fiber label-free biosensors, *ACS Sens.* 3 (5) (2018) 936–943.

**Adrián Vicente** obtained his degree of Electrical and Electronic engineering in 2016 and the Master of Industrial Engineering with Electronic Mention in 2018 from the Public University of Navarre (UPNA). His areas of interest are the optical fiber sensors and the development of optoelectronic devices.

**Desiree Santano Rivero** is a Biologist (2013) and received her M.Sc. in Microbiology and Health from the University of the Basque Country (UPV/EHU), Spain. She has co-authored conference papers related to Microbiology and Biomedical Engineering and other publications. Currently, she is working towards her PhD at PUN/UPNA. Her research interests focus on the biomedical engineering field, including the development of optical fibre biosensors.

**Pablo Zubiate** received his MS degree in Electrical and Electronic Engineering, the master's degree in communications and his Ph.D. degree in 2013, 2015 and 2018, respectively from the Public University of Navarre (UPNA). He has been working as visiting scientist at the school of Engineering of the University of East Anglia (Norwich, England) in 2018. He is a coauthor of 25 scientific papers. He has also participated in 10 different research projects and is a co-founder of the spin-off company PYROISTECH SL. Since 2019, he has been a postdoctoral position at Public University of Navarre. His research interest includes optical fiber sensors and nanostructured materials.

**Aitor Urrutia** received his PhD degree in Communication Technologies in 2015 from Public University of Navarre. He has been working as a visiting researcher in Dublin City University, and University of Nottingham. In 2016 he obtained a Postdoctoral Scholarship at Upna, and after a short stay at the University of Hull, he was working as a Postdoctoral Research Associate at The University of Birmingham. He is currently working as a Assistant Professor. He has coauthored 22 international publications in indexed journals and 29 national/international conference papers. His main areas of interests are the R&D in nanostructured functional coatings, optical fiber devices, sensors, and other engineering applications.

**Ignacio Del Villar** received the M.S. degree in electrical and electronic engineering and the Ph.D. degree, specialty in optical fiber sensors, in 2002 and 2006, respectively, from the Public University of Navarre (UPNA), Pamplona, Spain. During 2004, he was a visiting scientist with the Institute d'Optique, Orsay, France, and in 2005, he was a visiting scientist with the Applied Physics Department, University of Valencia, Burjassot, Spain. His research interest includes optical fiber sensors and the effect of nanostructured coatings deposited on waveguides, where he has coauthored more than 100 chapter books, journals, and conference papers. He has been a Reader with the UPNA since 2008, and an Associate Editor of the Optics & Laser Technology Journal since 2012 and of the MDPI Sensors Journal since 2017.

**C. R. Zamarreño** obtained his PhD in Communications from the Public University of Navarre (UPNA) in 2009, in 2012 he gained a Permanent position as Associate Professor at the UPNA and he has been working as visiting scientist at the MIT, Siemens, and UTFPR in 2008, 2011, 2013 and 2016 respectively. In 2013 he received the IEEE GOLD Award for his contributions to the development of novel optical sensing waveguides based on micro and nanostructured films where he has coauthored more than 100 scientific papers, most of them related to optical sensors based on Lossy Mode Resonances. He has also participated in 20 different research projects and is a co-founder of the spin-off company PYROISTECH SL.